
TTAQ: Towards Stable Post-training Quantization in Continuous Domain Adaptation

Junrui Xiao^{1,2}, Zhikai Li^{1,2}, Lianwei Yang^{1,2}, Yiduo Mei³, Qingyi Gu^{1*}

¹Institute of Automation, Chinese Academy of Sciences. Beijing, China

²School of Artificial Intelligence, University of Chinese Academy of Sciences. Beijing, China

³Inspur Yunzhou Industrial Internet Co., Ltd. Jinan City, Shandong Province, China

{xiaojunrui2020, qingyi.gu}@ia.ac.cn

Abstract

Post-training quantization (PTQ) reduces excessive hardware cost by quantizing full-precision models into lower bit representations on a tiny calibration set, without retraining. Despite the remarkable progress made through recent efforts, traditional PTQ methods typically encounter failure in dynamic and ever-changing real-world scenarios, involving unpredictable data streams and continual domain shifts, which poses greater challenges. In this paper, we propose a novel and stable quantization process for test-time adaptation (TTA), dubbed TTAQ, to address the performance degradation of traditional PTQ in dynamically evolving test domains. To tackle domain shifts in quantizer, TTAQ proposes the Perturbation Error Mitigation (PEM) and Perturbation Consistency Reconstruction (PCR). Specifically, PEM analyzes the error propagation and devises a weight regularization scheme to mitigate the impact of input perturbations. On the other hand, PCR introduces consistency learning to ensure that quantized models provide stable predictions for same sample. Furthermore, we introduce Adaptive Balanced Loss (ABL) to adjust the logits by taking advantage of the frequency and complexity of the class, which can effectively address the class imbalance caused by unpredictable data streams during optimization. Extensive experiments are conducted on multiple datasets with generic TTA methods, proving that TTAQ can outperform existing baselines and encouragingly improve the accuracy of low bit PTQ models in continually changing test domains. For instance, TTAQ decreases the mean error of 2-bit models on ImageNet-C dataset by an impressive 10.1%.

1 Introduction

In recent years, deep neural networks (DNNs) have achieved remarkable progress in various computer vision tasks, such as image classification Chen et al. [2021], Dosovitskiy et al. [2020], Lanchantin et al. [2021], object detection Carion et al. [2020], Xiao et al. [2022, 2023a], Liang et al. [2020], and semantic segmentation Strudel et al. [2021], Zheng et al. [2021], Liu et al. [2021a], thanks to the success of large-scale models trained on extremely large datasets. However, increasing demands for computation, memory, and storage present challenges in deploying these models in resource-limited devices or environments. Consequently, various model compression techniques have been proposed to address these resource constraints and accelerate inference, including pruning He et al. [2018], Yu et al. [2022], knowledge distillation Lin et al. [2022], Shi et al. [2020], Romero et al. [2015], Xu et al. [2022], structured factorization and quantization Li et al. [2022a,b], Liu et al. [2021c], Xiao et al. [2023b], Xu et al. [2023].

Model quantization has garnered significant attention as an effective technique that converts the weights and activations of large models from full-precision to low-bit fixed-point representations.

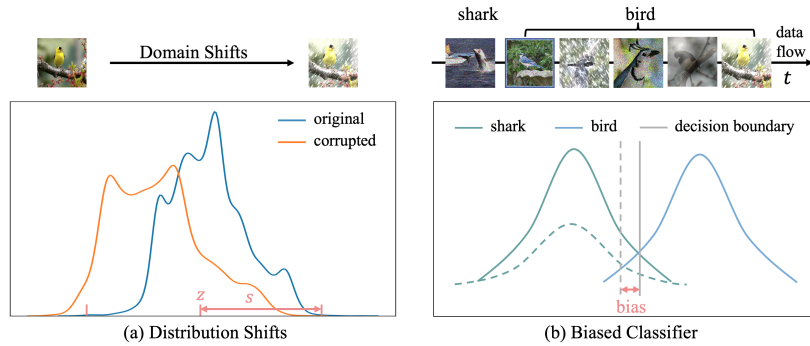


Figure 1: Illustration of the problem: (a) The distribution of the 1st to 10th channels of the activation in ResNet-18’s first convolutional layer shows a significant shift. The quantization parameters calibrated based on the original distribution are inaccurate, resulting in performance degradation; (b) A toy example illustrating the bias introduced by class-imbalanced samples. The solid gray line represents the unbiased classifier with the optimal decision boundary, while the dotted line depicts the learned biased classifier on imbalanced streaming samples, which also hinders the accuracy.

Most quantization works can be divided into two categories: quantization-aware training (QAT) Nagel et al. [2022], Choi et al. [2018], Esser et al. [2019] and post-training quantization (PTQ) Li et al. [2022b], Lin et al. [2021], Liu et al. [2021c], Yuan et al. [2022], Liu et al. [2021b]. By retraining the entire labeled dataset, QAT typically possesses higher accuracy but requires significant memory consumption and GPU efforts. On the contrary, PTQ only requires a tiny unlabeled calibration set to quantize the pre-trained parameters without retraining, and thus is regarded as a practical solution in widespread scenarios. Existing PTQ methods demonstrate great potential in terms of both accuracy and efficiency, as they can achieve good prediction accuracy on domain-invariant Wang et al. [2022a] test sets even when the quantized weights are reduced to 4 bits.

However, in real-world applications, domain shifts frequently occur at test-time due to corruptions, changes in weather conditions, camera sensor differences, and other factors. When there is an inconsistency between the distributions of the test and training data, the conventional PTQ method, which is calibrated on a fixed distribution, experiences severe performance degradation. Moreover, the data collected from edge devices, such as Internet of Things (IoT) products or wearable devices, arrives in a sequential manner, which presents additional challenges. This is due to the limited computational resources and the need for real-time processing, which makes it impractical to retrain all parameters using streaming data.

To perform online adaptation on the test stream characterized by an unpredictable distribution and provide instant predictions for incoming test samples, Continual Test-Time Adaptation (CTTA) Wang et al. [2022b], Gong et al. [2022], Döbler et al. [2023], Song et al. [2023] has emerged as a robust solution. CoTTA introduces an Exponentially Moving Average (EMA) Cai et al. [2021] teacher-student architecture to self-train all parameters using pseudo labels, which necessitates substantial memory during adaptation. To enhance efficiency, EATA Niu et al. [2022] employs an active sample selection criterion to identify reliable and non-redundant samples for updating the parameters of the batch normalization layer. However, current TTA approaches have focused primarily on full-precision models. The issue of *how to achieve stable quantization in CTTA* has not yet been explored thoroughly.

In this work, we first empirically reveal the potential problems of PTQ in the CTTA setting from two perspectives. Firstly, we observe that domain shifts directly cause alterations in the activation distribution, resulting in inaccurate calibrated quantization parameters (e.g., scale and zero point) and an increase in quantization errors, as illustrated in Figure 1(a). Secondly, when adapting on streaming data with an unpredictable distribution, imbalanced class distributions can easily arise, as shown in Figure 1(b), leading to a decrease in the model’s generalization capability and resulting in catastrophic forgetting of the minor class McCloskey and Cohen [1989].

Motivated by the analysis above, we propose a stable PTQ scheme in continuous domain adaptation, namely TTAQ, which considers both the robustness of quantization parameters and the imbalance

of classes in adaptation. First, we conduct an analysis of the error propagation stemming from perturbations, considering the signal-to-noise ratio, and then propose the Perturbation Error Mitigation (PEM), which introduces a weight-regularization scheme to mitigate the effect of input perturbations. Second, to further enhance the robustness, we propose Perturbation Consistent Reconstruction (PCR), which adds small perturbations during the block-wise reconstruction process and encourages quantized model can have the same output through perturbation consistency loss. Finally, we introduce Adaptive Balanced Loss (ABL) to address the class imbalance issue caused by unpredictable data streams. ABL reweights the samples based on class-wise frequency and adjusts logits by the accumulated gradients of each class, which effectively promotes the learning of unbiased classifiers.

We summarize our main contributions as follows:

- To the best of our knowledge, the proposed TTAQ is the first attempt to achieve stable post-training quantization in continuous domain adaptation by considering both quantization robustness and class imbalance.
- To enhance robust quantization, we introduce PEM and PCR, which effectively mitigate the impact of activation perturbations and improve prediction consistency.
- For addressing class imbalance, we propose ABL, which reweights samples based on class-wise factors that incorporate the frequency and complexity of each class.
- We conduct evaluations of TTAQ on various vision tasks, including image classification, object detection, and instance segmentation. Encouragingly, TTAQ demonstrates superior performance compared to existing PTQ approaches.

2 Related works

2.1 Model Quantization.

Model quantization Gholami et al. [2022], Nagel et al. [2021], Krishnamoorthi [2018] is one of the effective techniques for compressing and deploying neural networks, which quantizes the full-precision parameters to lower bit-width, and can be categorized as Quantization-Aware Training (QAT) and Post-Training Quantization (PTQ). QAT Nagel et al. [2022], Choi et al. [2018], Esser et al. [2019] shows the potential of low-precision computation by retraining the quantized model on a labeled training dataset. However, the time-consuming retraining and complex hyperparameters lead to limited applications. PTQ Li et al. [2022b], Lin et al. [2021], Liu et al. [2021c], Yuan et al. [2022], Liu et al. [2021b] stands out as an efficient and practical compression approach, as it directly quantizes the model without retraining. AdaroudNagel et al. [2020] introduces a continuous variable to each weight value to determine whether it should be rounded up or down, instead of using the nearest rounding. BrecqLi et al. [2021] first reconstructs the quantization parameters block by block and determines the step size for activation after the reconstruction stage. QDrop Wei et al. [2022] incorporates the activation error into the reconstruction process and introduces a drop operation to improve quantization. Pd-Quant Liu et al. [2023] argues that considering only local information leads to sub-optimal quantization parameters. Therefore, it proposes using the information of differences between network predictions before and after quantization to determine the quantization parameters.

Although existing PTQ models, which were calibrated on a fixed distribution of data, have achieved significant performance, it remains challenging to ensure their reliable prediction in dynamic environments. In particular, these environments are characterized by ever-changing streaming data.

2.2 Continual Test-time Adaptation.

In recent times, there has been a remarkable increase in research interest pertaining to test-time domain adaptation Wang et al. [2022b], Varsavsky et al. [2020], Gao et al. [2022] that adapts models during inference for addressing the domain shift problem. Test-time adaptation involves considering a fixed scenario where the test data are provided in batch format. NORM Mirza et al. [2021] adjusts the statistics of batch normalization (BN) layers using the current test samples, without updating other parameters. TENT Wang et al. [2020] introduces entropy minimization as a test-time optimization objective. SAR Niu et al. [2023] proposes a reliable and sharpness-aware entropy minimization method to remain robust in the presence of large and noisy gradients. Continual test-time adaptation is a scenario where the target domain is dynamic with a stream of continually changing samples,

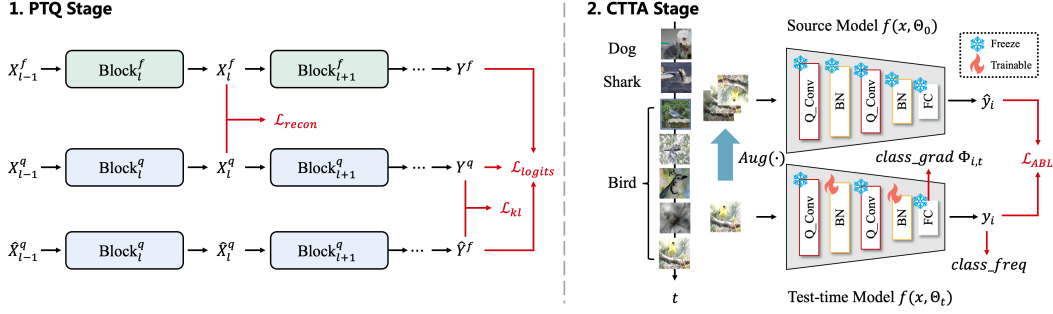


Figure 2: Pipeline of TTAQ. In Post-Training Quantization stage (left), perturbation consistency reconstruction apply consistency learning by encouraging quantized model can have the same output when there is a slight perturbation between X_{l-1}^q and \hat{X}_{l-1}^q . TTAQ also introduce global information by \mathcal{L}_{logits} to alleviate the overfitting problem. In Continual Test-Time Adaption stage (right), adaptive balanced loss adjusts the logits by the frequency and accumulated gradient of each class to enhance the learning of unbiased classifiers.

presenting increased challenges for traditional computer vision tasks. CoTTA Wang et al. [2022b] employs weighted averaging, improved average prediction, and random parameter recovery to prevent catastrophic forgetting. EcoTTA Song et al. [2023] introduces a small meta-network to regularize the outputs from both the meta-network and the frozen network. RMT Döbler et al. [2023] introduces a symmetric cross-entropy loss through gradient analysis. RoIDMarsden et al. [2024] defines all relevant settings as universal TTA and then proposes a model-agnostic certainty and diversity weighting.

In this paper, our aim is to achieve a stable and efficient PTQ under a continual every-changing domain, without the need for additional prompts or adapters.

3 Method

In this section, we introduce the proposed TTAQ in detail. To reduce the perturbation from domain shifts, we propose perturbation error mitigation and perturbation consistency reconstruction, respectively, as detailed in Section 3.2 and Section 3.3. To address the class imbalance of unpredictable streaming data, we propose adaptive balanced loss in Section 3.4. The overview of TTAQ is shown in Figure 2.

3.1 Preliminaries

Overview of CTTA. In this work, our focus lies on the continuous adaptation environment during testing time, where access to the source data is not available during adaptation. Here, the pre-trained model must adapt to an unlabeled and continuously changing target domain in an online manner. First, consider a model $f(x_i; \Theta) \in \mathbb{R}^{H \times W \times C}$ trained using data $D_{\text{source}} = \{(x_i, y_i)\}_{i=1}^N$, where (x_i, y_i) denote the image and label i_{th} drawn from the source distribution D_{source} , respectively. Now, deploy the pre-trained model $f(x_i; \Theta)$ to the test environments where the test data at inference time T is $D_{\text{target}}^T = \{x_j\}_{j=1}^B$, and D_{target}^T deviates from the i.i.d. assumption. Our goal is to adapt the model $f(\cdot; \Theta_t)$ to $f(\cdot; \Theta_{t+1})$ using only the unlabeled input x_j^T while making predictions directly. Following previous CTTA methods Niu et al. [2022], Marsden et al. [2024], we freezes the majority of the model’s parameters, permitting only minor adjustments for efficient adaptation.

Scheme of PTQ. Post-training quantization (PTQ) leverages a subset of unlabeled images to determine the scaling factors s and zero point z of activations and weights for each layer. For convenience, we revisit the uniform quantization. Uniform quantization quantizes the weights or activation values from full precision X to integer X^q when given a quantization bit width b . The processes quantization

and dequantization are shown as follows:

$$Quant : \mathbf{X}^q = \text{clamp} \left(\left\lfloor \frac{\mathbf{X}}{s} \right\rfloor + z, 0, 2^b - 1 \right) \quad (1)$$

$$DeQuant : \mathbf{X}^{dq} = s \left(\mathbf{x}^{(Z)} - z \right) \approx \mathbf{x} \quad (2)$$

where $\lfloor \cdot \rfloor$ represents the round function, clamp limits the range of values to between 0 and $2^b - 1$. s and z can be calculated as:

$$s = \frac{\max(\mathbf{X}) - \min(\mathbf{X})}{2^b - 1}, \quad z = \left\lfloor -\frac{\min(\mathbf{X})}{s} \right\rfloor. \quad (3)$$

Block-wise Nagel et al. [2020], Wei et al. [2022] reconstruction is proposed to further to minimize the quantization error of PTQ. In this work, we also employ the block-wise reconstruction as the learning objective. For the l_{th} block of the full-precision model and quantized model, we achieve this by minimizing the error between the block outputs. The process can be formulated as:

$$\arg \min_{s_l} \mathcal{L}_{recon}(X_l^f, X_l^q) \quad (4)$$

where the X_l^f and X_l^q represent the output of the l_{th} block of the full-precision model and the quantized model, respectively.

3.2 Perturbation Error Mitigation

In this section, we detail perturbation error mitigation. Following EATA Niu et al. [2022], we adapt the model only by updating the parameters in the Batch Norm layer instead of the whole model to prioritize efficiency for edge devices. However, during adaptation to the changing target domain, the distribution of the input to the PTQ model will change (as shown in Figure 1(a)), and the quantization parameters cannot be updated, resulting in the layer-by-layer accumulation of quantization errors. As revealed in Table 1, we also conduct a experiment to show that the performance of the PTQ model degrades more under the CTTA setting.

To address the above issues, we first conduct an analysis of the error propagation resulting from perturbations Meller et al. [2019], Park et al. [2022]. Consider a convolutional layer with kernel $W_{(K_x \cdot K_y \cdot F_{in}) \times F_{out}}^{i,j}$, input $x_{1 \times (K_x \cdot K_y \cdot F_{in})}^j$, and output $y_{1 \times F_{out}}^i$. For notional simplicity we model both convolution and linear operation as matrix multiplication and model the domain shift as $g(\cdot)$:

$$y_i = \sum_j^N W_{i,j} g(x_j) \quad (5)$$

where $W_{i,j}$ is an arbitrary and fixed value, and $g(x_j)$ represents a corrupted activation assumed to be an i.i.d. variable. When quantizer $Q(\cdot)$ is applied to the weight, the output can be formulated as:

$$\hat{y}_i = \sum_j^N Q(W_{i,j}) g(x_j) \quad (6)$$

We use signal noise ratio to compute the effect of the input perturbation:

$$SNR_{y_i} = \frac{E_i[(\hat{y}_i - y_i)^2]}{E_i[y_i^2]} \quad (7)$$

where y_i and \hat{y}_i denote the i_{th} output with the full-precision weight $W_{i,j}$ and quantized weight $Q(W_{i,j})$, respectively. Since the $E_i[y_i^2]$ term is constant for i_{th} layer, the optimization objective is to minimize the $E_i[(\hat{y}_i - y_i)^2]$.

$$\arg \min_{Q(\cdot)} E_i[(\hat{y}_i - y_i)^2] = \arg \min_{Q(\cdot)} (E_i[(\hat{y}_i - y_i)])^2 + Var(\hat{y}_i - y_i) \quad (8)$$

Let $\mathbb{E}(g(x_i)) = \mu_g$ and $\text{Var}(g(x_i)) = \sigma_g^2$, the expected value and the variance of output y_i can be expressed as:

$$\mathbb{E}_i(y_i) = N \mu_g \mathbb{E}_i(W_{i,j}), \quad \text{Var}_i(y_i) = N \sigma_g^2 \mathbb{E}_i(W_{i,j}^2) \quad (9)$$

Table 1: Mean Error (%) of Quantized ResNet-18 He et al. [2015] with different bit-widths on ImageNet-C Hendrycks and Dietterich [2019]. CTTA Error represents the performance degradation of the PTQ Model in CTTA setting, while Quant Error represents the performance degradation of the PTQ Model in the source domain compared to FP model. As is evident, there is an extra degradation caused by inaccurately calibrated quantization parameters.

Method	Bit	Mean	CTTA Error	Quant Error	Extra Error
TENT	FP	69.69	-	-	-
	W4A4	75.69	-6	-4.03	-2.03
	W2A4	80.86	-12.83	-10	-2.83
EATA	FP	65.9	-	-	-
	W4A4	72.8	-6.9	-4.03	-1.87
	W2A4	78.12	-12.22	-10	-2.22

It is straightforward to show that the optimization objective in Eq. 8 can be rewritten as:

$$\arg \min_{Q(\cdot)} [\mathbb{E}_i(Q(W_{i,j})) - \mathbb{E}_i(W_{i,j})]^2 + [\mathbb{E}_i(Q(W_{i,j})^2) - \mathbb{E}_i(W_{i,j}^2)] \quad (10)$$

However, rigorously solving the final objective in Eq. 10 becomes challenging since PTQ only conducts a simple parameter space search with a limited calibration set. To ease the difficulty, we adopt the additional condition as given by:

$$\mathbb{E}_i(Q(W_{i,j})) = \mathbb{E}_i(W_{i,j}), \quad \mathbb{E}_i(Q(W_{i,j})^2) = \mathbb{E}_i(W_{i,j}^2) \quad (11)$$

To this end, we can mitigate perturbation error by regularizing the distribution of weights to satisfy Eq. 11. Inspired by the crucial role of normalization in quantization Li et al. [2019], Banner et al. [2018], Chen et al. [2023], we devise a weight regularization scheme:

$$Q(\hat{W}_{i,j}) = Q\left(\alpha \cdot \frac{W_{i,j} - \mu_{W_{i,\cdot}}}{\sigma_{W_{i,\cdot}}}\right) \quad (12)$$

where the mean $\mu_{W_{i,\cdot}}$ and variance $\sigma_{W_{i,\cdot}}$ are computed by $\mu_{W_{i,\cdot}} = \frac{1}{N} \sum_j W_{i,j}$ and $\sigma_{W_{i,\cdot}}^2 = \frac{1}{N} \sum_j W_{i,j}^2 - \mu_{W_{i,\cdot}}^2$, while α is a fixed constant. By recalling Eq. 11, we can find that $\mathbb{E}_i(Q(\hat{W}_{i,j})) = \mathbb{E}_i(\hat{W}_{i,j}) = 0$ and $\mathbb{E}_i(Q(\hat{W}_{i,j})^2) = \mathbb{E}_i(\hat{W}_{i,j}^2)$. Note that, due to regularization depends on the fixed parameters rather than dynamic activations, we can use weight re-parameterization to keep efficiency during inference.

3.3 Perturbation Consistency Reconstruction

Following QDrop Wei et al. [2022], we employ block-wise reconstruction to determining quantization parameters by minimizing the feature distance before and after quantization. However, PD-quant Liu et al. [2023] points out that such an approach, which only considers local information, is prone to overfitting to the calibration samples. Moreover, randomly dropping the quantized activations during PTQ and using fully quantized activations during inference will cause unnegligible inconsistency between calibration and inference.

We first introduce a global objective based on the analysis in Liu et al. [2023] to mitigate the overfitting:

$$\arg \min_s \mathcal{L}_{logits}(f(X_0^f), f_{l+1}(B_l^q(X_{l-1}^q))) \quad (13)$$

where B_l^q represents the block being reconstructed, $f_{l+1}(\cdot)$ is the part that has not been quantified yet, $f(X_0^f)$ is FP output, and X_0^f and X_{l-1}^q denote input sample and the quantized feature from the previous reconstructed Block.

To further encourage the model to generate consistent predictions between the original and perturbed features, we propose perturbation consistency reconstruction loss. Specifically, we introduce a random perturbation ϵ_l to input feature X_l^q of l_{th} block. The classifier will output two prediction of the original feature X_l^q and perturbed feature $\hat{X}_l^q = X_l^q + \epsilon_l$, denoted as $f_{l+1}(B_l^q(X_{l-1}^q))$ and $f_{l+1}(B_l^q(\hat{X}_{l-1}^q))$.

We use Kullback-Leibler (KL) divergence as the objection to constrain the predicted probability of the perturbed features to be consistent with the original features, which can be formulated as:

$$\arg \min_s \mathcal{L}_{kl}(f_{l+1}(B_l^q(X_{l-1}^q)), f_{l+1}(B_l^q(\hat{X}_{l-1}^q))) \quad (14)$$

Combining Eq. 13 and Eq. 14 and , we obtain perturbation consistency reconstruction loss:

$$\begin{aligned} \mathcal{L}_{pcr} = & \frac{1}{2} [\mathcal{L}_{logits}(f(X_0^f), f_{l+1}(B_l^q(X_{l-1}^q))) \\ & + \mathcal{L}_{logits}(f(X_0^f), f_{l+1}(B_l^q(\hat{X}_{l-1}^q)))] \\ & + \mathcal{L}_{kl}(f_{l+1}(B_l^q(X_{l-1}^q)), f_{l+1}(B_l^q(\hat{X}_{l-1}^q))) \end{aligned} \quad (15)$$

In actual implementation, excessively aggressive perturbations may result in significant differences between the predicted distributions of the original features and the perturbed features, thus causing the consistency constraint to fail. Therefore, careful selection of the perturbation strategy is necessary.

3.4 Adaptive Balanced Loss

In Section 3.2 and Section 3.3, we propose PEM and PCR to enable the PTQ models to remain robust under minor perturbations in dynamic and ever-changing real-world scenarios. However, since the model needs to adapt online to sequentially arriving data, imbalanced class distributions can easily arise, resulting in catastrophic forgetting and unstable learning. Recent TTA research Niu et al. [2022], Marsden et al. [2024] is proposed to address the forgetting issue by employing sample reweighting for accuracy enhancement without considering class imbalance issue.

To mitigate the impact of inter-class imbalance, we propose an adaptive balanced loss (ABL) to adjust the logits in loss during prediction. Unlike approaches Zhao et al. [2023], Marsden et al. [2024], ABL considers not only the frequency, but also the accumulated gradients of each class. Motivated by Menon et al. [2020], He and Zhu [2024], we adjust the logits in ABL to achieve reweighting as follows:

$$\mathcal{L}_{ABL}(y_i) = -\log \frac{e^{y_i + \log \pi_{y_i, t}}}{\sum_{j=1}^{|\mathcal{Y}^1|} e^{y_j + \log \pi_{y_j, t}}} \quad (16)$$

where \mathcal{Y}^1 denotes class labels, and $\pi_{y, t}$ is the class prior $\mathbb{P}(y | \mathcal{S}_t)$ at time t . To tackle the dynamically changing and unknown input data stream, we use a momentum-updated class-wise vector, which is initiated with $\pi = [\pi^1, \dots, \pi^C]$, to store the corresponding class-prior. To this end, we compute class-prior $\pi_{y, t}$ by:

$$\pi_{y_i, t} = \frac{\overbrace{\sum_{y \in |\mathcal{Y}^1|} \mathbf{1}(y_i = \mathcal{Y}^1)}^{\text{class frequency}}}{C} \cdot \frac{\overbrace{\Phi_{i, t}}^{\text{class gradient}}}{\sum_{j=1}^{|\mathcal{Y}^1|} \Phi_{j, t}} \quad (17)$$

$$\text{where } \Phi_{i, t} = \sum_{n=1}^i \|\nabla \mathcal{L}_{ce}(W_n)\|$$

where $\mathbf{1}(\cdot)$ is the indicator function of label y_i to count the frequency of each category, and $\Phi_{i, t}$ is the accumulated gradients of i_{th} class, which is computed from the fully connected layer.

4 Experiment

In this section, we review the our TTAQ on several benchmark tasks to validate the effectiveness of our approach.

4.1 Experimental Setup

Datasets. For the image classification task, we employ CIFAR10, CIFAR100, and ImageNet Rusakovsky et al. [2015] as the source domain datasets, and CIFAR10-C, CIFAR100-C, and ImageNet-C/K Hendrycks and Dietterich [2019] as the respective target domain datasets. These target domain

datasets are designed to evaluate the robustness of classification networks, with each containing 15 types of corruption at 5 severity levels. For the object detection task, we generate a corrupted version of COCO, labeled COCO-C, following the approach outlined in Michaelis et al. [2019], which introduces 15 types of corruptions.

Models and Implementation details. All pretrained full precision models are obtained from `torchvision`. In the PTQ stage, we randomly sample 1024 images from the ImageNet training dataset as the calibration set. We maintain the same quantization settings and hyperparameters in our implementation as QDrop Wei et al. [2022]. In the CTTA stage, we follow Wang et al. [2020], Niu et al. [2022], Marsden et al. [2024] to utilize a quantized W2A4 WideResNet Zagoruyko and Komodakis [2016] and ResNeXt Xie et al. [2017] for CIFAR10-to-CIFAR10-C and CIFAR100-to-CIFAR100-C, respectively. For the ImageNet-to-ImageNet-C dataset, we employ quantized ResNet He et al. [2016] with different bit widths for a comprehensive comparison.

Table 2: Ablation study of PEM, PCR, and ABL is presented. All results for the continual test-time adaptation task are evaluated in ImageNet-C, with the largest corruption severity level 5.

Time	t															Mean
	<i>Gaussian</i>	<i>shot</i>	<i>impulse</i>	<i>defocus</i>	<i>glass</i>	<i>motion</i>	<i>zoom</i>	<i>snow</i>	<i>frost</i>	<i>fog</i>	<i>brightness</i>	<i>contrast</i>	<i>elastic</i>	<i>pixelate</i>	<i>jpeg</i>	
Baseline	77.06	66.96	64.88	75.14	70.78	63.66	54.54	57.18	61.80	47.88	36.76	70.54	49.10	46.06	49.20	59.44
+PEM	74.28	64.02	63.50	73.70	69.36	62.22	53.60	55.66	61.64	46.50	36.12	70.00	47.78	44.76	47.40	58.04
+PEM+PCR	73.60	64.30	63.40	73.88	69.22	61.08	53.22	55.40	61.20	46.78	36.10	69.62	48.00	44.14	47.64	57.88
+PEM+PCR+ABL	73.12	62.62	63.18	74.68	68.92	61.26	53.08	56.22	60.90	46.56	35.56	68.60	47.92	44.74	47.62	57.67

4.2 Ablation Study

To validate the efficiency and effectiveness of the proposed components, we report the classification error of W4A4 ResNet-50 on the ImageNet-to-ImageNet-C task with highest corruption severity level 5. As shown in Table 2, we set the models quantized by QDrop and adapted by Tent as baseline and sequentially incorporate each of our contributions to better understand their individual effects on performance. Compared to the strong baseline, our TTAQ reduce the mean error by approximately 1.77%. Specifically, when PEM is applied, the model to get 58.04% mean error in W4A4 which is 1.4% lower than the model quantized by qdrop. Further, the addition of the PCR reduced the model’s average error rate from 58.04% to 57.88%, and when combined ABL, the average error further down to 57.67%.

4.3 Comparison on Classification Task

Results on ImageNet-C and ImageNet-K. As shown in Table 3, we evaluate ResNet-18 and ResNet-50 models with different bit-widths and PTQ methods on various corrupted datasets. It is evident that the performance of traditional PTQ is highly sensitive to continuous domain variations. For instance, when the bit-width is W2A2, the average error of ResNet-50 on the ImageNet-C dataset increases by 29.95% and 29.97% for Brecq and QDrop respectively, while Adaround fails to predict in this setting altogether. In comparison, TTAQ achieves a reduction of 9% and 8.82% in average error compared to Brecq and QDrop, respectively. Furthermore, the issue of quantization parameter overfitting, as described in Section 3.3, is more pronounced in ResNet-50, which shows that the accuracy of W2A2 is even lower than that of R-18. However, our TTAQ method mitigates this problem and ensures a stable prediction across different models.

Results on Cifar100-C and Cifar10-C. As presented in Table 4, we evaluate the performance on CIFAR100-C and CIFAR10-C using quantized ResNext and WideResNet models with W2A4 bit-width. We also provide a detailed the average error rate for each corruption type. In CIFAR100-C, our TTAQ approach consistently outperforms the traditional PTQ method across all corruption types, resulting in an average error rate of 32.45%, which is lower compared to the other three methods, with reductions of 1.78%, 2.03%, and 1.17% respectively. Similarly, in CIFAR10-C, our method demonstrates superior performance on most corruption types, resulting in an average error rate of 17.04%. Additionally, as shown in Figure 3, we provided t-SNE visualizations of the baselines and our method. The results demonstrated that the proposed TTAQ approach generated more discriminative features.

Table 3: Classification error rate (%) for the ImageNet-to-ImageNet-C and ImageNet-to-ImageNet-K online continual test-time adaptation task on the highest corruption severity level 5.

Method	ResNet-50 on IN-C				ResNet-18 on IN-C				ResNet-50 on IN-K			
	W4A4	W3A3	W2A4	W2A2	W4A4	W3A3	W2A4	W2A2	W4A4	W3A3	W2A4	W2A2
Adaround	59.08	66.88	69.48	*	66.34	70.46	72.57	*	67.02	73.30	76.65	*
Brecq	59.64	69.46	67.53	89.59	66.45	72.26	71.07	84.82	66.98	74.56	73.83	89.83
QDrop	59.44	67.11	66.20	89.41	66.35	71.57	70.46	84.37	66.53	71.52	72.68	89.66
TTAQ (ours)	57.67	62.89	62.05	80.59	65.17	69.49	68.99	82.71	66.24	69.91	69.52	83.80

Table 4: Classification error rate (%) for the CIFAR100-to-CIFAR100C, CIFAR10-to-CIFAR10C online continual test-time adaptation task on the highest corruption severity level 5.

Dataset	Time	$t \rightarrow$													Mean		
	Method	Gaussian	Shot	Impulse	Defocus	Glass	motion	Zoom	Snow	Frost	Fog	Brightness	Contrast	Elastic		Pixelate	Jpeg
Cifar100-C	Full precision	36.31	31.89	33.36	25.13	35.00	27.05	24.22	28.95	28.85	31.63	23.14	23.55	30.81	27.05	34.10	29.41
	Adaround	39.30	35.52	38.07	31.76	38.93	32.47	29.43	33.81	33.49	36.78	27.20	36.13	35.40	30.73	36.56	34.35
	Brecq	40.26	35.48	38.23	31.84	38.87	32.40	29.56	33.81	33.44	37.04	27.37	36.58	35.62	31.47	37.49	34.73
	QDrop	40.44	35.37	37.68	31.53	39.16	32.31	29.32	33.75	33.10	36.58	27.19	36.63	35.58	30.79	37.07	34.53
	TTAQ (ours)	37.75	33.95	35.56	29.59	37.86	30.67	28.07	31.68	31.66	34.72	25.54	34.01	33.90	29.60	35.81	32.73
Cifar10-C	Full precision	23.62	18.41	26.14	11.71	27.95	12.32	9.80	14.91	14.33	11.99	7.42	9.31	19.75	14.30	20.41	16.20
	Adaround	24.34	19.30	26.25	13.81	28.59	14.06	12.12	16.12	15.46	13.47	8.40	13.50	20.91	15.34	20.25	17.46
	Brecq	24.31	19.22	26.12	14.23	28.41	14.16	12.19	15.76	15.07	13.33	8.30	13.63	20.23	15.48	19.77	17.43
	QDrop	24.34	18.99	26.04	14.03	28.26	13.88	12.09	15.67	14.78	13.30	8.22	13.48	20.91	15.65	19.67	17.31
	TTAQ (ours)	24.32	18.63	27.05	13.28	29.27	13.37	11.08	14.80	14.72	13.24	8.09	12.00	20.42	14.69	20.48	17.08

Table 5: Mean Average Precision (%) for the COCO-to-COCO-C online continual test-time adaptation task on the corruption severity level 1-5.

#Bits	Time	$t \rightarrow$													mAP		
	Method	Gaussian	Shot	Impulse	Defocus	Glass	motion	Zoom	Snow	Frost	Fog	Brightness	Contrast	Elastic		Pixelate	Jpeg
FP	-	12.05	12.02	9.74	12.78	8.10	11.28	5.59	12.64	15.56	20.68	21.82	15.36	15.14	9.54	10.68	12.86
W4A4	Adaround	4.63	4.57	3.02	3.91	2.73	4.45	2.07	4.47	5.47	6.47	11.00	3.77	7.86	3.47	4.85	8.85
	Brecq	10.48	10.51	8.50	10.44	7.63	9.89	4.69	11.64	13.94	16.04	20.62	13.94	14.57	9.33	11.67	11.32
	QDrop	10.85	10.94	9.03	10.47	7.65	10.14	4.81	11.43	13.93	16.84	20.70	10.74	14.38	9.59	11.53	11.54
	TTAQ (ours)	10.94	11.15	9.14	11.23	7.67	10.44	4.99	11.97	14.39	17.63	21.21	11.59	14.71	9.72	11.24	11.87
W2A4	Adaround	4.46	4.60	3.26	4.87	3.85	4.80	2.24	5.25	7.12	6.47	11.44	3.58	7.92	4.63	5.49	5.33
	Brecq	6.80	7.00	5.34	6.97	5.82	6.94	3.07	7.70	9.89	10.74	16.28	5.88	12.29	7.28	9.21	8.08
	QDrop	7.30	7.36	5.60	7.41	5.97	7.45	3.23	8.04	10.09	11.93	16.78	6.97	12.13	7.12	8.70	8.41
	TTAQ (ours)	9.31	9.33	7.46	9.90	6.38	8.86	3.95	10.21	12.69	15.23	19.00	9.62	12.92	8.55	9.99	10.23

4.4 Comparison on Object Detection Task

The experimental results of the object detection task, which conducted on the COCO-C dataset with the Faster RCNN framework, are reported in Table 5. We set the quantized ResNet-50 with W4A4 and W2A4 bit-width as the backbone, while keeping other components in full precision. In the W4A4 bit-width setting, our method outperforms Brecq and QDrop by 0.55% and 0.33% mAP, respectively. Furthermore, in the W2A4 bit-width setting, our method demonstrates an improvement in performance over Brecq and QDrop by 2.15% and 1.82% mAP, respectively. Similar to the results in the classification task, our method maintains a more stable performance even at lower bit-widths.

5 Conclusion

In this paper, we introduce TTAQ, a novel approach for stable post-training quantization in continuous domain adaptation. TTAQ incorporates Perturbation Error Mitigation, which analyzes error propagation based on signal-to-noise ratio and implements a weight regularization scheme to minimize the impact of input perturbations. Additionally, TTAQ introduces Perturbation Consistent Reconstruction

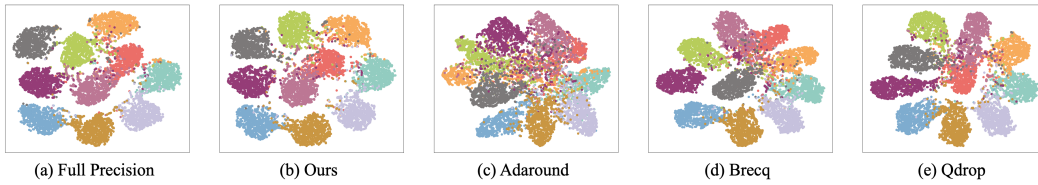


Figure 3: T-SNE visualization of learned feature on quantized wider-resnet (W2A4), which reveal discriminative capability of classifier.

to ensure consistent predictions when there is a small perturbation in calibration. Furthermore, Adaptive Balanced Loss is proposed to address class imbalance by adjusting sample weights according to class-wise factors, thereby enhancing the learning of unbiased classifiers. Exhaustive experiments across various vision tasks validate the superiority of TTAQ, demonstrating significant performance improvements over existing PTQ methods in continuous domain adaptation.

References

- Ron Banner, Yury Nahshan, Elad Hoffer, and Daniel Soudry. Acicq: Analytical clipping for integer quantization of neural networks. *ArXiv*, 2018.
- Zhaowei Cai, Avinash Ravichandran, Subhransu Maji, Charles Fowlkes, Zhuowen Tu, and Stefano Soatto. Exponential moving average normalization for self-supervised and semi-supervised learning. In *Proceedings of the IEEE/CVF Conference on Computer Vision and Pattern Recognition*, pages 194–203, 2021.
- Nicolas Carion, Francisco Massa, Gabriel Synnaeve, Nicolas Usunier, Alexander Kirillov, and Sergey Zagoruyko. End-to-end object detection with transformers. In *Proc. of ECCV*, pages 213–229, 2020.
- Chun-Fu (Richard) Chen, Quanfu Fan, and Rameswar Panda. Crossvit: Cross-attention multi-scale vision transformer for image classification. In *Proc. of ICCV*, pages 347–356, 2021.
- Ting-An Chen, De-Nian Yang, and Ming-Syan Chen. Overcoming forgetting catastrophe in quantization-aware training. *Proc. of ICCV*, 2023.
- Jungwook Choi, Zhuo Wang, Swagath Venkataramani, Pierce I-Jen Chuang, Vijayalakshmi Srinivasan, and Kailash Gopalakrishnan. Pact: Parameterized clipping activation for quantized neural networks. *arXiv preprint arXiv:1805.06085*, 2018.
- Mario Döbler, Robert A Marsden, and Bin Yang. Robust mean teacher for continual and gradual test-time adaptation. In *Proceedings of the IEEE/CVF Conference on Computer Vision and Pattern Recognition*, pages 7704–7714, 2023.
- Alexey Dosovitskiy, Lucas Beyer, Alexander Kolesnikov, Dirk Weissenborn, Xiaohua Zhai, Thomas Unterthiner, Mostafa Dehghani, Matthias Minderer, Georg Heigold, Sylvain Gelly, et al. An image is worth 16x16 words: Transformers for image recognition at scale. *arXiv preprint arXiv:2010.11929*, 2020.
- Steven K Esser, Jeffrey L McKinstry, Deepika Bablani, Rathinakumar Appuswamy, and Dharmendra S Modha. Learned step size quantization. *arXiv preprint arXiv:1902.08153*, 2019.
- Yunhe Gao, Xingjian Shi, Yi Zhu, Hao Wang, Zhiqiang Tang, Xiong Zhou, Mu Li, and Dimitris N Metaxas. Visual prompt tuning for test-time domain adaptation. *arXiv preprint arXiv:2210.04831*, 2022.
- Amir Gholami, Sehoon Kim, Zhen Dong, Zhewei Yao, Michael W Mahoney, and Kurt Keutzer. A survey of quantization methods for efficient neural network inference. In *Low-Power Computer Vision*, pages 291–326. Chapman and Hall/CRC, 2022.
- Taesik Gong, Jongheon Jeong, Taewon Kim, Yewon Kim, Jinwoo Shin, and Sung-Ju Lee. Note: Robust continual test-time adaptation against temporal correlation. *Advances in Neural Information Processing Systems*, 35:27253–27266, 2022.
- Jiangpeng He and Fengqing Zhu. Gradient reweighting: Towards imbalanced class-incremental learning. *ArXiv*, 2024.
- Kaiming He, X. Zhang, Shaoqing Ren, and Jian Sun. Deep residual learning for image recognition. *Proc. of CVPR*, 2015.
- Kaiming He, Xiangyu Zhang, Shaoqing Ren, and Jian Sun. Identity mappings in deep residual networks. In *Proc. of ECCV*. Springer, 2016.
- Yang He, Guoliang Kang, Xuanyi Dong, Yanwei Fu, and Yi Yang. Soft filter pruning for accelerating deep convolutional neural networks. In *Proc. of IJCAI*, pages 2234–2240, 2018.
- Dan Hendrycks and Thomas G. Dietterich. Benchmarking neural network robustness to common corruptions and perturbations. *Proc. of ICLR*, 2019.
- Raghuraman Krishnamoorthi. Quantizing deep convolutional networks for efficient inference: A whitepaper. *arXiv preprint arXiv:1806.08342*, 2018.

- Jack Lanchantin, Tianlu Wang, Vicente Ordonez, and Yanjun Qi. General multi-label image classification with transformers. In *Proc. of CVPR*, pages 16478–16488, 2021.
- Yanjing Li, Sheng Xu, Baochang Zhang, Xianbin Cao, Peng Gao, and Guodong Guo. Q-vit: Accurate and fully quantized low-bit vision transformer. In *Proc. of NeurIPS*, 2022a.
- Yuhang Li, Xin Dong, and Wei Wang. Additive powers-of-two quantization: An efficient non-uniform discretization for neural networks. *arXiv preprint arXiv:1909.13144*, 2019.
- Yuhang Li, Ruihao Gong, Xu Tan, Yang Yang, Peng Hu, Qi Zhang, Fengwei Yu, Wei Wang, and Shi Gu. Brecq: Pushing the limit of post-training quantization by block reconstruction. *arXiv preprint arXiv:2102.05426*, 2021.
- Zhikai Li, Junrui Xiao, Lianwei Yang, and Qingyi Gu. Repq-vit: Scale reparameterization for post-training quantization of vision transformers. *arXiv preprint arXiv:2212.08254*, 2022b.
- Xi Liang, Jing Zhang, Li Zhuo, Yuzhao Li, and Qi Tian. Small object detection in unmanned aerial vehicle images using feature fusion and scaling-based single shot detector with spatial context analysis. *IEEE Transactions on Circuits and Systems for Video Technology*, 30:1758–1770, 2020.
- Sihao Lin, Hongwei Xie, Bing Wang, Kaicheng Yu, Xiaojun Chang, Xiaodan Liang, and Gang Wang. Knowledge distillation via the target-aware transformer. In *Proc. of CVPR*, pages 10905–10914, 2022.
- Yang Lin, Tianyu Zhang, Peiqin Sun, Zheng Li, and Shuchang Zhou. Fq-vit: Fully quantized vision transformer without retraining. *arXiv preprint arXiv:2111.13824*, 2021.
- Jiawei Liu, Lin Niu, Zhihang Yuan, Dawei Yang, Xinggang Wang, and Wenyu Liu. Pd-quant: Post-training quantization based on prediction difference metric. In *Proceedings of the IEEE/CVF Conference on Computer Vision and Pattern Recognition*, pages 24427–24437, 2023.
- Weide Liu, Guosheng Lin, Tianyi Zhang, and Zichuan Liu. Guided co-segmentation network for fast video object segmentation. *IEEE Transactions on Circuits and Systems for Video Technology*, 31:1607–1617, 2021a.
- Zhenhua Liu, Yunhe Wang, Kai Han, Siwei Ma, and Wen Gao. Post-training quantization for vision transformer. In *Proc. of NeurIPS*, 2021b.
- Zhenhua Liu, Yunhe Wang, Kai Han, Wei Zhang, Siwei Ma, and Wen Gao. Post-training quantization for vision transformer. In *Proc. of NeurIPS*, pages 28092–28103, 2021c.
- Robert A Marsden, Mario Döbler, and Bin Yang. Universal test-time adaptation through weight ensembling, diversity weighting, and prior correction. In *Proceedings of the IEEE/CVF Winter Conference on Applications of Computer Vision*, pages 2555–2565, 2024.
- Michael McCloskey and Neal J. Cohen. Catastrophic interference in connectionist networks: The sequential learning problem. *Psychology of Learning and Motivation*, 1989.
- Eldad Meller, Alexander Finkelstein, Uri Almog, and Mark Grobman. Same, same but different: Recovering neural network quantization error through weight factorization. 2019.
- Aditya Krishna Menon, Sadeep Jayasumana, Ankit Singh Rawat, Himanshu Jain, Andreas Veit, and Sanjiv Kumar. Long-tail learning via logit adjustment. *Proc. of ICML*, 2020.
- Claudio Michaelis, Benjamin Mitzkus, Robert Geirhos, Evgenia Rusak, Oliver Bringmann, Alexander S. Ecker, Matthias Bethge, and Wieland Brendel. Benchmarking robustness in object detection: Autonomous driving when winter is coming. *ArXiv*, 2019.
- M. Jehanzeb Mirza, Jakub Micorek, Horst Possegger, and Horst Bischof. The norm must go on: Dynamic unsupervised domain adaptation by normalization. *Proc. of CVPR*, 2021.
- Markus Nagel, Rana Ali Amjad, Mart Van Baalen, Christos Louizos, and Tijmen Blankevoort. Up or down? adaptive rounding for post-training quantization. In *International Conference on Machine Learning*, pages 7197–7206. PMLR, 2020.

- Markus Nagel, Marios Fournarakis, Rana Ali Amjad, Yelysei Bondarenko, Mart Van Baalen, and Tijmen Blankevoort. A white paper on neural network quantization. *arXiv preprint arXiv:2106.08295*, 2021.
- Markus Nagel, Marios Fournarakis, Yelysei Bondarenko, and Tijmen Blankevoort. Overcoming oscillations in quantization-aware training. In Kamalika Chaudhuri, Stefanie Jegelka, Le Song, Csaba Szepesvári, Gang Niu, and Sivan Sabato, editors, *Proc. of ICML*, volume 162, pages 16318–16330, 2022.
- Shuaicheng Niu, Jiayang Wu, Yifan Zhang, Yafo Chen, Shi Dong Zheng, Peilin Zhao, and Mingkui Tan. Efficient test-time model adaptation without forgetting. 2022.
- Shuaicheng Niu, Jiayang Wu, Yifan Zhang, Zhiquan Wen, Yafo Chen, Peilin Zhao, and Mingkui Tan. Towards stable test-time adaptation in dynamic wild world. *arXiv preprint arXiv:2302.12400*, 2023.
- Sein Park, Yeongsang Jang, and Eunhyeok Park. Symmetry regularization and saturating nonlinearity for robust quantization. *Proc. of ECCV*, 2022.
- Adriana Romero, Nicolas Ballas, Samira Ebrahimi Kahou, Antoine Chassang, Carlo Gatta, and Yoshua Bengio. Fitnets: Hints for thin deep nets. In *Proc. of ICLR*, pages 1–13, 2015.
- Olga Russakovsky, Jia Deng, Hao Su, Jonathan Krause, Sanjeev Satheesh, Sean Ma, Zhiheng Huang, Andrej Karpathy, Aditya Khosla, Michael Bernstein, Alexander C. Berg, and Li Fei-Fei. Imagenet large scale visual recognition challenge. *International Journal of Computer Vision*, 115(3):211–252, 2015. ISSN 1573-1405.
- Jun Shi, Jianfeng Xu, Kazuyuki Tasaka, and Zhibo Chen. Sasl: Saliency-adaptive sparsity learning for neural network acceleration. *IEEE Transactions on Circuits and Systems for Video Technology*, 31:2008–2019, 2020.
- Junha Song, Jungsoo Lee, In So Kweon, and Sungha Choi. Ecotta: Memory-efficient continual test-time adaptation via self-distilled regularization. In *Proceedings of the IEEE/CVF Conference on Computer Vision and Pattern Recognition*, pages 11920–11929, 2023.
- Robin Strudel, Ricardo Garcia Pinel, Ivan Laptev, and Cordelia Schmid. Segmenter: Transformer for semantic segmentation. In *Proc. of ICCV*, pages 7242–7252, 2021.
- Thomas Varsavsky, Mauricio Orbes-Arteaga, Carole H Sudre, Mark S Graham, Parashkev Nachev, and M Jorge Cardoso. Test-time unsupervised domain adaptation. In *Medical Image Computing and Computer Assisted Intervention—MICCAI 2020: 23rd International Conference, Lima, Peru, October 4–8, 2020, Proceedings, Part I 23*, pages 428–436. Springer, 2020.
- Dequan Wang, Evan Shelhamer, Shaoteng Liu, Bruno Olshausen, and Trevor Darrell. Tent: Fully test-time adaptation by entropy minimization. *arXiv preprint arXiv:2006.10726*, 2020.
- Fan Wang, Zhongyi Han, Yongshun Gong, and Yilong Yin. Exploring domain-invariant parameters for source free domain adaptation. In *Proceedings of the IEEE/CVF Conference on Computer Vision and Pattern Recognition*, pages 7151–7160, 2022a.
- Qin Wang, Olga Fink, Luc Van Gool, and Dengxin Dai. Continual test-time domain adaptation. In *Proceedings of the IEEE/CVF Conference on Computer Vision and Pattern Recognition*, pages 7201–7211, 2022b.
- Xiuying Wei, Ruihao Gong, Yuhang Li, Xianglong Liu, and Fengwei Yu. Qdrop: Randomly dropping quantization for extremely low-bit post-training quantization. *arXiv preprint arXiv:2203.05740*, 2022.
- Junrui Xiao, He Jiang, Zhikai Li, and Qingyi Gu. Rethinking prediction alignment in one-stage object detection. *Neurocomputing*, 514:58–69, 2022.
- Junrui Xiao, He Jiang, Zhikai Li, and Qingyi Gu. Dcifpn: Deformable cross-scale interaction feature pyramid network for object detection. *IET Image Processing*, 2023a.

- Junrui Xiao, Zhikai Li, Lianwei Yang, and Qingyi Gu. Patch-wise mixed-precision quantization of vision transformer. 2023b.
- Saining Xie, Ross Girshick, Piotr Dollár, Zhuowen Tu, and Kaiming He. Aggregated residual transformations for deep neural networks. In *Proc. of CVPR*, 2017.
- Sheng Xu, Yanjing Li, Bohan Zeng, Teli Ma, Baochang Zhang, Xianbin Cao, Peng Gao, and Jinhu Lu. Ida-det: An information discrepancy-aware distillation for 1-bit detectors. *arXiv preprint arXiv:2210.03477*, 2022.
- Weixiang Xu, Fanrong Li, Yingying Jiang, A Yong, Xiangyu He, Peisong Wang, and Jian Cheng. Improving extreme low-bit quantization with soft threshold. *IEEE Transactions on Circuits and Systems for Video Technology*, 33:1549–1563, 2023.
- Fang Yu, Kun Huang, Meng Wang, Yuan Cheng, Wei Chu, and Li Cui. Width & depth pruning for vision transformers. In *Proc. of AAAI*, pages 3143–3151, 2022.
- Zhihang Yuan, Chenhao Xue, Yi-Qiang Chen, Qiang Wu, and Guangyu Sun. Ptq4vit: Post-training quantization for vision transformers with twin uniform quantization. In *Proc. of ECCV*, 2022.
- Sergey Zagoruyko and Nikos Komodakis. Wide residual networks. In *Proc. of BMVC*, 2016.
- Bowen Zhao, Chen Chen, and Shutao Xia. Delta: degradation-free fully test-time adaptation. *Proc. of ICLR*, 2023.
- Sixiao Zheng, Jiachen Lu, Hengshuang Zhao, Xiatian Zhu, Zekun Luo, Yabiao Wang, Yanwei Fu, Jianfeng Feng, Tao Xiang, Philip H. S. Torr, and Li Zhang. Rethinking semantic segmentation from a sequence-to-sequence perspective with transformers. In *Proc. of CVPR*, pages 6881–6890, 2021.